

User Provided Data Products of Herschel/PACS photometric light curve measurements of trans-Neptunian objects and Centaurs

Release Note, Version 1.0, November 23, 2017

Cs. Kiss¹, G. Marton¹, T. Müller², V. Ali-Lagoa²

¹ Konkoly Observatory, Research Centre for Astronomy and Earth Sciences,
Hungarian Academy of Sciences, Budapest, Hungary

² Max-Planck-Institut für extraterrestrische Physik, Garching, Germany

Abstract

In this release note we describe the delivery of User Provided Data Products (UPDPs) of thermal emission light curve measurements of Centaurs and trans-Neptunian objects, observed in scan-map mode with the PACS photometer cameras of the Herschel Space Observatory. We discuss light curve observations of (136199) Eris, (50000) Quaoar, (20000) Varuna, (136108) Haumea, 84922 (2003 VS2), 208996 (2003 AZ84), (2060) Chiron and (134340) Pluto. These UPDPs combined data of multiple epochs. They were reduced with an optimized pipeline, corrections were applied for an optimal background elimination and a careful quality check was performed for all measurements. We could also make a partial recovery of the failed Eris measurements from OD807, which was caused by an SPU failure. In addition to the light curve targets we provide background corrected data products for the extreme Centaur 2012 DR30. Altogether we provide 3972 FITS products.

Contents

| | | |
|---|---|-----------|
| 1 | Introduction | 2 |
| 2 | Data reduction of light curve observations | 2 |
| 3 | Data products provided as UPDPs | 3 |
| 4 | Comments on specific light curve targets | 4 |
| 4.1 | Eris (OT1_evilenui_1) | 4 |
| 4.2 | Quaoar (OT1_evilenui_1) | 5 |
| 4.3 | Varuna (KPOT_thmuelle_1) | 5 |
| 4.4 | Haumea (KPOT_thmuelle_1) | 5 |
| 4.5 | 2003 VS2 (KPOT_thmuelle_1) | 5 |
| 4.6 | 2003 AZ84 (KPOT_thmuelle_1) | 6 |
| 4.7 | Chiron (DDT_mustdo_3) | 6 |
| 4.8 | Pluto (OT2_elellouc_2) | 6 |
| 4.9 | 'TNOs are Cool!' -type data products of 2012 DR30 and 2013 AZ60 | 6 |
| References | | 9 |
| Appendix | | 10 |
| Summary of additional FITS keywords | | 10 |
| List of data products provided with this release note | | 11 |

1 Introduction

This document describes the delivery of User Provided Data Products (UPDPs) of selected observations of Centaurs and trans-Neptunian objects, taken with the PACS photometer cameras (Poglitsch et al., 2010) of the Herschel Space Observatory (Pilbratt et al., 2010). The main aim of most of these observation were to obtain thermal emission light curves. The observations were taken in the framework of the proposal/programs 'TNOs are Cool! – A Survey of the trans-Neptunian region' Herschel Open Time Key Program (Müller et al., 2009); the Open Time Program 'Probing the extremes of the outer Solar System: short-term variability of the largest, the densest and the most distant TNOs from PACS photometry' (OT1_evileniu_1, PI: E. Vilenius) and the DDT proposal 'The thermal lightcurve of Centaur (2060) 95P/Chiron' (DDT_mustdo_3; PI: E. Lellouch). We cover observations of the targets (136199) Eris, (50000) Quaoar, (20000) Varuna, (136108) Haumea, 84922 (2003 VS2), 208996 (2003 AZ84), (2060) Chiron and (134340) Pluto.

In an earlier delivery of UPDPs of Centaurs and trans-Neptunian objects (Kiss et al., 2017), combined data products of multiple epoch observations of 132 targets were delivered to the Herschel Science Archive. There, only those targets that complied strictly with the 'TNOs are Cool!' Open Time Key program standard observing strategy and combined data product requirements were included .

In this delivery we also investigate Herschel/PACS measurements of two targets, 2012 DR30 and 2013 AZ60 that comply with the standards of the 'TNOs are Cool!' observing and data reduction strategies, but were not included in the earlier 'TNOs are Cool!' delivery, as they were obtained in two DDT programs: DDT_ckiss_2 ("2012 DR 30: A wanderer from the far edges of the Solar System", PI: Cs. Kiss) and DDT_ckiss_3 ("The 'supercomet' candidate 2013 AZ60", PI: Cs. Kiss). For the details of the data reduction and the detailed description of the products we refer to the 'TNOs are Cool!' UPDP release note (Kiss et al., 2017). Data reduction is further described in a dedicated paper (Kiss et al., 2014).

We apply a reduction pipeline optimized for faint, slow-moving targets, and use specific methods to correct for possible pointing and positional uncertainties, as described below.

2 Data reduction of light curve observations

Herschel/PACS TNO and Centaur light curve measurements are scan-map measurements using the same observing configuration in up to ~ 100 repetitions over the target, lasting up to ~ 8 h in a single OBSID. Currently the Standard Product Generation (SPG) of the Herschel Science Archive (HSA) does not provide products that could be used for light curve determination as in the HSA SPG products all repetitions are merged into a single image. In this delivery we provide products in which the long measurements are split into smaller sections by selecting repetitions from the scan-map sequence (for a detailed description of the observing mode, see the PACS Observer's Manual¹). In the case of the blue detector (70 and $100\ \mu\text{m}$) we use 3-repetition images, while for the red detector ($160\ \mu\text{m}$) we provide images both with 3 and 6 repetitions. Note that most of these products are provided with overlapping repetitions – e.g. in the case of 3-repetition images the shift between two subsequent images in only one repetition. It is up to the user of these products to consider this. Some of the Eris UPDPs were produced without overlapping repetitions, using 10 repetitions per product, as discussed below.

For the main data reduction we use a modified version of the PACS pipeline for basic data reduction of scan-maps, producing single images per OBSID, from raw data to Level-2 maps (for the definition of the Herschel/PACS data product levels, see the PACS Observer's Manual). Raw data were obtained from the Herschel Science Archive (SPG v14.2.0) and we used Herschel Interactive Processing Environment (HIPE, Ott 2010) version 15.0.0 (RC2) for data reduction. We applied the following main parameters in HIPE (for a summary of the PACS photometer scan-maps calibration, see Balog et al., 2014):

- Raw data and auxiliary information are obtained directly from the HSA via the getObservation() task.
- Slews are selected on scan speed with a limit parameter of $limits=10$, i.e. between 15 and $25''\ \text{s}^{-1}$ for $20''\ \text{s}^{-1}$ scan speed. We note that only measurements with $20''\ \text{s}^{-1}$ speed were considered for our UPDPs.

¹http://herschel.esac.esa.int/Docs/PACS/html/pacs_om.html

- High-pass filter widths of 8, 9 and 16 readouts are used at 70, 100 and 160 μm , respectively – (high pass filter width sets the number of frames [2n+1] used for median subtraction from the detector timeline; see Popesso et al., 2012 and Balog et al., 2014, for a detailed description of the method).
- Masking pixels above 2-sigma, and at the source position with 2xFWHM radius
- We apply second level deglitching with nsigma=30, the sigma-clipping parameter of this deglitching method working on the map level (see the PACS Data Reduction Guide for more details).

Signal drift correction via the `scanamorphosBaselinePreprocessing()` task can be applied on the data in two ways, either using a fit algorithm (`forceFitSubtraction=True`) or simply masking the first frames of the observations. When the second option (`forceMasking=True`) is applied to typical scan map observations of faint targets, a significant part of the measurement is lost, which results in a too low signal-to-noise ratio for the final maps. Therefore we do not use this option for scan map observations.

We apply the drizzle method to project the time-line data and produce the single maps using the `photProject()` task in HIPE, with a pixel fraction parameter of 1.0.

We use pixel sizes of 1''/1, 1''/4 and 2''/1 in the PACS 70, 100 and 160 μm bands, respectively, which allows an optimal sampling of the respective point spread functions. As our targets are Centaurs and trans-Neptunian objects their typical apparent speeds are low, and the displacements are usually negligible within a given observation section. Therefore, a specific motion correction is *not* applied in our pipeline – this is also an important requirement for an optimal background elimination, an essential step in the detection of faint targets (see below). A detailed description of the data reduction pipeline can be found in Kiss et al. (2014).

3 Data products provided as UPDPs

The list of Herschel/PACS TNO and Centaur thermal emission light curve targets and their typical flux density levels in the Herschel/PACS photometric bands can be found in Table 1. A list of all light curve target observations is given in Table 2.

The main light curve images that can be used for photometry are called 'LCMAIN' in our nomenclature, as it appears in the file names of the respective products. Here the map is obtained by using a set of repetitions selected from the respective OBSID, reduced in the fixed sky frame, and without applying background correction. Typically we provide LCMAIN products using 3 repetitions for the blue detector (70 or 100 μm) and 3 and 6 repetitions for the red detector (160 μm) data. In the case of very faint targets (e.g. Eris) there are data products with a different number of repetitions used, as described below.

In all cases either the thermal light curve measurements is repeated in a few days providing mutual backgrounds for the first and second visits due to the apparent movement of the target, or a dedicated background (or 'shadow') observation is executed, when the target has already moved away from the light curve field. For this purpose, all measurements are reduced as well in a way that ALL repetitions are used and merged into a single image. These 'backgrounds' are called 'LCALL' products in the case of mutual backgrounds (when both measurements are light curve measurements as well on their own) and 'LCBG' products, when a dedicated background is used, without the presence of the target in the field. In both cases, these images are solely used for background correction. However, the average flux density of the target can indeed be extracted from the LCALL data. In addition to the main light curve products we provide background corrected ('LCDIFF') images for all light curve measurements, whenever it is possible, using these 'background' products, made of the LCMAIN images with the corresponding LCALL/LCBG image subtracted.

In some cases a light curve measurement was followed by a 'follow-on' measurement sequence, typically two-by-two measurements with the 70/160 and 100/160 filter combinations. In these cases the main products are the mosaics of the images of the individual OBSIDs of the same band, two at 70, two at 100 and four at 160 μm . These combined products are referred to as 'LCB1', 'LCG1' and 'LCR1' for the 70, 100, and 160 μm bands, respectively. In the case of follow-on measurements these 'LC?1' products are used instead of an LCALL or LCBG product to provide background subtraction for the corresponding 'LCDIFF' image.

File naming of the data product FITS (and JPEG thumbnail) images is described in Fig. 1.

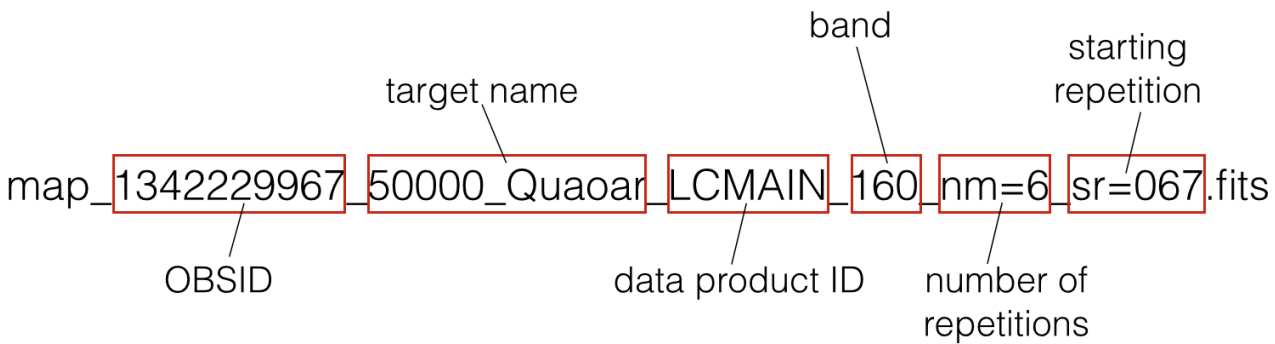


Figure 1: Demonstration of file naming convention for a typical FITS file. The file name contains the OBSID, the target name, the data product ID, the band/wavelength of the observation (μm), the number of repetitions used for this specific product, and the ID of the starting repetition. In the case of combined images of follow-on measurements the file name simply contains the target name and the product ID ('LCB1', 'LCG1' or 'LCR1').

The structure of data products is somewhat different from the scheme above for some Eris measurements. In these cases an instrument anomaly of the PACS blue detector prevented us from producing standard light curve products for the OBSIDs 1342224854/55. Details are discussed below in Sect. 4.

Below we describe the data products that are provided for the light curve measurements in the current UPDP release. A specific product is identified by:

- the Herschel observation identifier (OBSID)
- the target name, which is a combination of the name, number, and/or provisional designation, e.g. "2060_Chiron"
- a data product ID: 'LCMAIN', 'LCDIFF', 'LCALL' or 'LC[B,G,R]1', as described above
- the Herschel/PACS band used
- for LCMAIN and LCDIFF products the number of repetitions (nm=) and starting repetitions (sr=)

All these parameters are provided as FITS keywords as well (see the list of FITS keywords in the Appendix).

The FITS files contain a FITS cube with two layers, the first layer being the image itself (LAYER0) and the second layer being the coverage information (LAYER1). Note that in the case of background-subtracted images (LCDIFF) high coverage areas may be those where the background image had high coverage values, due to the sometimes longer integration in the subtracted image than in the primary one.

We provide the start and end dates (see the FITS keywords 'JDSTART' and 'JD_END') of the time interval covered by the selected repetitions, in Julian date format.

As no apparent motion correction is applied, the WCS information in the FITS files is correct for main images, and also in the background-corrected ones, as long as the features of the main image are considered. The list of data products provided can be found in the Appendix.

4 Comments on specific light curve targets

4.1 Eris (OT1_evilenui_1)

In the case of OBSIDs 1342224854 and 1342224855 there was an instrument anomaly that prevents the proper reduction of these observations with the optimized pipeline and production of standard light curve products.

Most of the blue detector ($100\mu\text{m}$) data of the OBSID 1342224854 is lost, only the first 23 repetitions (of the 60) could be recovered. The blue channel data ($70\mu\text{m}$) of the OBSID 1342224855 are completely lost. The red channel data, however, could be fully recovered for both OBSIDs.

For the red channel data of the OBSIDs 1342224854/55 we provide light curves with background subtraction, using the co-added image of the OBSIDs 1342238741/42 as background (*map_1342238741_1342238742_Eris_Background_LCBG_160.fits*, see below). These are 10-repetition maps, starting with the first repetition of each OBSID, with *no overlap* in repetitions between the maps. The corresponding files are *map_13422248[54,55]_136199_Eris_LCDIFF_160_nm=10_sr=[001,011,021,031,041,051].fits*.

Due to the faintness of the target and the complexity of the background (many faint sources around the target at $160\mu\text{m}$) we do not provide light curve products without background correction here.

In addition to the $160\mu\text{m}$ light curve of the OBSIDs 1342224854/55 we provide a single map for the blue channel part ($100\mu\text{m}$) of the OBSID 1342224854, using the first 23 repetitions. This is a stacked image, background subtracted (using the background map *map_1342238741_1342238742_Eris_Background_LCBG_100.fits*, see below) and then corrected for the apparent motion of Eris. The final images is stored in the file *map_1342224854.136199_Eris_STACKED_100_nm=23_sr=001.fits*.

OBSIDs 1342225116/17/18/19 are the follow-on observations of the failed measurements, presently the related HSA/SPG products sufficiently cover them. These are *not* used as backgrounds for any Eris thermal light curve measurements.

OBSIDs 1342238741/42 are background measurements for the failed observations 1342224854/55. While the corresponding HSA/SPG products (both high-pass filter/photProject and JS-CANAM maps) sufficiently cover these OBSIDs we provide the combined, co-added maps (*map_1342238741_1342238742_Eris_Background_LCBG_[100,160].fits*) in both the 100 and $160\mu\text{m}$ bands, as these were used for background correction, as mentioned above. We note that the observation 1342238741 was executed shortly after the detector bias setting that might have lead to a small response drift of the detector. However, this effect has not been seen in the data .

OBSIDs 1342238743/44 and 1342238863/64 are mutual background pairs, and we used the corresponding image with the same scan angle (70° or 110°) for background correction, i.e. using the pairs 1342238743–1342238863 and 1342238744–1342238864 when producing LCDIFF images.

4.2 Quaoar (OT1_evileniu_1)

Three observations with equal length (82 repetitions each) and partial background overlap were executed, using the $100/160$ filter combination. We used the 2nd measurement as the 1st measurement's background when producing the LCDIFF files, and the 2nd and 3rd measurements as mutual backgrounds. Note the mismatch between the sequence of the measurements and the OBSIDs that was caused by a later re-scheduling of previously failed observations.

4.3 Varuna (KPOT_thmuelle_1)

OBSIDs 1342218722 and 1342219023 are used as mutual background when producing LCDIFF products.

4.4 Haumea (KPOT_thmuelle_1)

OBSIDs 1342188470 and 1342188520 are used as mutual background when producing LCDIFF products. Combined data products (LC?1) from the OBSIDs 1342198903/04/05/06 are used as backgrounds for 1342198851.

4.5 2003 VS2 (KPOT_thmuelle_1)

Combined data products (LC[B,G,R]1) from the OBSIDs 1342202574/75/76/77 are used as backgrounds for 1342202371.

Table 1: Light curve targets: flux levels in each band, rotation period, visual amplitude, combination of n map repetitions for an individual thermal lightcurve data point with sufficient signal-to-noise ratio (smaller number is referring to the shorter wavelength channels where the target is usually brighter, larger number for the red channel).

| Number/ Name | | Approx. flux level [mJy] at | | | P_{sid} [hours] | Δmag in V-band | Rep. for LC | Remarks |
|-----------------|--------------------------|-----------------------------|-------------------|-------------------|----------------------|---------------------------------|----------------|-----------------|
| | | 70 μm | 100 μm | 160 μm | | | | |
| 2 060 | Chiron | 54 | 46 | 24 | 5.9 | 0.1 | 1- 6 | |
| 20 000 | Varuna | 8 | 9 | 6 | 6.3 | 0.4 | 5-10 | |
| 50 000 | Quaoar | 32 | 41 | 30 | 8.8-18.8 | 0.1-0.3 | 1- 4 | binary |
| 84 922 | (2003 VS ₂) | 14 | 16 | 12 | 3.7-7.4 | 0.2 | 4-10 | |
| 134 340 | Pluto | 280 | 370 | 340 | 153.3 | 0.3 | 1 | multiple system |
| 136 108 | Haumea | 17 | 21 | 20 | 2.0-3.9 | 0.3 | 2- 5 | multiple system |
| 136 199 | Eris | 2 | 4 | 5 | 3.6-28.1 | 0.1 | 10-15 | binary |
| 208 996 | (2003 AZ ₈₄) | 28 | 25 | 17 | 6.7-13.6 | 0.1 | 2- 5 | binary |

4.6 2003 AZ84 (KPOT_thmuelle_1)

Combined data products (LC?1) from the OBSIDs 1342205222/23/24/25 are used as backgrounds for 1342205152.

4.7 Chiron (DDT_mustdo_3)

OBSID 1342257513 is used as a background/shadow measurements for the long light curve measurement of 1342257765.

4.8 Pluto (OT2_elellouc_2)

All 'lightcurve-like' Pluto measurements were executed in separate OBSIDs and are single repetition measurements, therefore the apparent motion-corrected HSA/SPG images provide sufficient products for light curve photometry.

4.9 'TNOs are Cool!' -type data products of 2012 DR30 and 2013 AZ60

Observations of the extreme Centaur 2012 DR30 (OBSIDs 1342246148/49/50/51 and 1342246215/16/17/18) followed the same scheme as the TNO and Centaur observations of the 'TNOs are Cool!' Open Time Key Program (see Kiss et al., 2014, 2017). Consequently, these observations have been combined to produce background corrected (DIFF and DDIFF) products, following the data reduction scheme described in Kiss et al. (2014, 2017). The data products provided along with this release note are listed in the Appendix. A detailed discussion of these data can also be found in Kiss et al. (2013).

A similar set of observations were executed for another extreme Centaur, 2013 AZ60. However, the position of the target was not well known at the time of the observation due to the very short orbital arc then available. This resulted in a significant offset of the target and the image centre at both observational epochs (OBSIDs 1342268974/75/76/77 and 1342268990/91/92/93), and preventing us from producing combined data products (DIFF and DDIFF) images. For a more detailed discussion we refer to the dedicated scientific paper by Pál et al. (2015). The respective, single epoch standard data products in the Herschel Science Archive are sufficient for the photometry of the target.

Table 2: Herschel-PACS photometer scan-map observations for the light curve targets (see also tables in the appendix). All data are taken in "large scan" observing mode, high gain, SSO tracking (except the Eris and Chiron background measurements), satellite scan speed: always $20''/\text{s}$. SAA: solar aspect angle; Dur.: duration of observation in seconds; Fil.: filter/band combination (B: $70/160\ \mu\text{m}$; G: $100/160\ \mu\text{m}$); Rep: repetition of entire scan map; scan-map parameters: scan-leg length (in arc min) \times number of scan legs \times scan-leg separation (in arc sec); angle: satellite scan angle in degrees with respect to instrument reference frame.

| OD | OBSID | Target | SAA | UTC Start time | Dur. | Fil. | Rep. | ScanLeg \times n \times cross | angle |
|------|------------|---------------------------------|-------|----------------------|-------|------|------|-----------------------------------|-------|
| 807 | 1342224854 | 136199 Eris | -13.1 | 2011 Jul 29 19:22:24 | 17348 | G | 60 | $3.0' \times 10 \times 4.0''$ | 110 |
| 807 | 1342224855 | 136199 Eris | -13.3 | 2011 Jul 30 00:08:46 | 15263 | B | 60 | $3.0' \times 10 \times 4.0''$ | 110 |
| 810 | 1342225116 | 136199 Eris | -15.9 | 2011 Aug 01 22:55:52 | 1175 | G | 2 | $3.0' \times 10 \times 4.0''$ | 110 |
| 810 | 1342225117 | 136199 Eris | -16.0 | 2011 Aug 01 23:11:09 | 603 | G | 2 | $3.0' \times 10 \times 4.0''$ | 70 |
| 810 | 1342225118 | 136199 Eris | -16.1 | 2011 Aug 01 23:21:40 | 603 | B | 2 | $3.0' \times 10 \times 4.0''$ | 110 |
| 810 | 1342225119 | 136199 Eris | -16.1 | 2011 Aug 01 23:32:11 | 603 | B | 2 | $3.0' \times 10 \times 4.0''$ | 70 |
| 1000 | 1342238741 | Bgr of Eris | 25.1 | 2012 Feb 07 14:47:09 | 6747 | G | 23 | $3.0' \times 10 \times 4.0''$ | 110 |
| 1000 | 1342238742 | Bgr of Eris | 25.1 | 2012 Feb 07 16:38:03 | 6525 | G | 23 | $3.0' \times 10 \times 4.0''$ | 70 |
| 1000 | 1342238743 | 136199 Eris | 26.2 | 2012 Feb 07 18:08:17 | 4268 | B | 15 | $3.0' \times 10 \times 4.0''$ | 110 |
| 1000 | 1342238744 | 136199 Eris | 26.2 | 2012 Feb 07 19:19:54 | 4268 | B | 15 | $3.0' \times 10 \times 4.0''$ | 70 |
| 1002 | 1342238863 | 136199 Eris | 28.0 | 2012 Feb 09 13:56:21 | 4388 | B | 15 | $3.0' \times 10 \times 4.0''$ | 110 |
| 1002 | 1342238864 | 136199 Eris | 28.0 | 2012 Feb 09 15:08:58 | 4268 | B | 15 | $3.0' \times 10 \times 4.0''$ | 70 |
| 871 | 1342229967 | 50000 Quaoar | 17.7 | 2011 Oct 01 22:15:48 | 23558 | G | 82 | $3.0' \times 10 \times 4.0''$ | 110 |
| 873 | 1342230064 | 50000 Quaoar | 19.6 | 2011 Oct 03 21:39:02 | 23818 | G | 82 | $3.0' \times 10 \times 4.0''$ | 110 |
| 872 | 1342230111 | 50000 Quaoar | 18.7 | 2011 Oct 02 22:06:35 | 23767 | G | 82 | $3.0' \times 10 \times 4.0''$ | 110 |
| 703 | 1342218722 | 20000 Varuna | 6.2 | 2011 Apr 17 05:49:51 | 14218 | G | 51 | $2.5' \times 10 \times 4.0''$ | 110 |
| 705 | 1342219023 | 20000 Varuna | 8.1 | 2011 Apr 19 05:26:57 | 14102 | G | 51 | $2.5' \times 10 \times 4.0''$ | 110 |
| 223 | 1342188470 | 136108 Haumea | 14.3 | 2009 Dec 23 07:31:24 | 12119 | G | 40 | $3.5' \times 10 \times 4.0''$ | 63 |
| 225 | 1342188520 | 136108 Haumea | 12.6 | 2009 Dec 25 06:32:29 | 2454 | G | 8 | $3.5' \times 10 \times 4.0''$ | 63 |
| 403 | 1342198851 | 136108 Haumea | -14.2 | 2010 Jun 20 22:52:57 | 15548 | G | 55 | $3.0' \times 10 \times 4.0''$ | 70 |
| 404 | 1342198903 | 136108 Haumea | -13.4 | 2010 Jun 21 22:45:14 | 603 | B | 2 | $3.0' \times 10 \times 4.0''$ | 110 |
| 404 | 1342198904 | 136108 Haumea | -13.3 | 2010 Jun 21 22:55:45 | 603 | B | 2 | $3.0' \times 10 \times 4.0''$ | 70 |
| 404 | 1342198905 | 136108 Haumea | -13.3 | 2010 Jun 21 23:06:16 | 603 | G | 2 | $3.0' \times 10 \times 4.0''$ | 110 |
| 404 | 1342198906 | 136108 Haumea | -13.3 | 2010 Jun 21 23:16:47 | 603 | G | 2 | $3.0' \times 10 \times 4.0''$ | 70 |
| 453 | 1342202371 | 84922 (2003 VS ₂) | 20.6 | 2010 Aug 10 13:28:56 | 25415 | B | 100 | $3.0' \times 10 \times 4.0''$ | 110 |
| 454 | 1342202574 | 84922 (2003 VS ₂) | 20.1 | 2010 Aug 11 03:05:49 | 603 | B | 2 | $3.0' \times 10 \times 4.0''$ | 110 |
| 454 | 1342202575 | 84922 (2003 VS ₂) | 20.1 | 2010 Aug 11 03:16:20 | 603 | B | 2 | $3.0' \times 10 \times 4.0''$ | 70 |
| 454 | 1342202576 | 84922 (2003 VS ₂) | 20.1 | 2010 Aug 11 03:26:51 | 603 | G | 2 | $3.0' \times 10 \times 4.0''$ | 110 |
| 454 | 1342202577 | 84922 (2003 VS ₂) | 20.1 | 2010 Aug 11 03:37:22 | 603 | G | 2 | $3.0' \times 10 \times 4.0''$ | 70 |
| 501 | 1342205152 | 208996 (2003 AZ ₈₄) | 22.3 | 2010 Sep 27 03:35:03 | 26828 | G | 95 | $3.0' \times 10 \times 4.0''$ | 110 |
| 502 | 1342205222 | 208996 (2003 AZ ₈₄) | 21.3 | 2010 Sep 28 02:54:21 | 603 | B | 2 | $3.0' \times 10 \times 4.0''$ | 110 |
| 502 | 1342205223 | 208996 (2003 AZ ₈₄) | 21.4 | 2010 Sep 28 03:04:52 | 603 | B | 2 | $3.0' \times 10 \times 4.0''$ | 70 |
| 502 | 1342205224 | 208996 (2003 AZ ₈₄) | 21.3 | 2010 Sep 28 03:15:23 | 603 | G | 2 | $3.0' \times 10 \times 4.0''$ | 110 |
| 502 | 1342205225 | 208996 (2003 AZ ₈₄) | 21.3 | 2010 Sep 28 03:25:54 | 603 | G | 2 | $3.0' \times 10 \times 4.0''$ | 70 |
| 1316 | 1342257513 | Bgr of Chiron | 22.4 | 2012 Dec 19 20:05:06 | 3123 | B | 8 | $2.5' \times 14 \times 4.0''$ | 110 |
| 1322 | 1342257765 | 2060 Chiron | 28.3 | 2012 Dec 25 17:05:18 | 24182 | B | 88 | $2.5' \times 10 \times 4.0''$ | 110 |
| 1035 | 1342241381 | Pluto | 15.3 | 2012 Mar 14 03:00:45 | 496 | B | 1 | $3.0' \times 10 \times 4.0''$ | 110 |
| 1035 | 1342241382 | Pluto | 15.3 | 2012 Mar 14 03:08:02 | 321 | B | 1 | $3.0' \times 10 \times 4.0''$ | 70 |
| 1035 | 1342241383 | Pluto | 15.4 | 2012 Mar 14 03:13:51 | 321 | G | 1 | $3.0' \times 10 \times 4.0''$ | 110 |
| 1035 | 1342241384 | Pluto | 15.3 | 2012 Mar 14 03:19:40 | 321 | G | 1 | $3.0' \times 10 \times 4.0''$ | 70 |
| 1035 | 1342241418 | Pluto | 14.6 | 2012 Mar 14 19:53:41 | 474 | B | 1 | $3.0' \times 10 \times 4.0''$ | 110 |
| 1035 | 1342241419 | Pluto | 14.6 | 2012 Mar 14 20:00:47 | 321 | B | 1 | $3.0' \times 10 \times 4.0''$ | 70 |
| 1035 | 1342241420 | Pluto | 14.7 | 2012 Mar 14 20:06:36 | 321 | G | 1 | $3.0' \times 10 \times 4.0''$ | 110 |
| 1035 | 1342241421 | Pluto | 14.6 | 2012 Mar 14 20:12:25 | 321 | G | 1 | $3.0' \times 10 \times 4.0''$ | 70 |
| 1036 | 1342241471 | Pluto | 13.9 | 2012 Mar 15 12:57:33 | 476 | B | 1 | $3.0' \times 10 \times 4.0''$ | 110 |
| 1036 | 1342241472 | Pluto | 13.9 | 2012 Mar 15 13:04:40 | 321 | B | 1 | $3.0' \times 10 \times 4.0''$ | 70 |
| 1036 | 1342241473 | Pluto | 14.0 | 2012 Mar 15 13:10:29 | 321 | G | 1 | $3.0' \times 10 \times 4.0''$ | 110 |
| 1036 | 1342241474 | Pluto | 13.9 | 2012 Mar 15 13:16:18 | 321 | G | 1 | $3.0' \times 10 \times 4.0''$ | 70 |
| 1037 | 1342241509 | Pluto | 13.2 | 2012 Mar 16 06:33:04 | 455 | B | 1 | $3.0' \times 10 \times 4.0''$ | 110 |
| 1037 | 1342241510 | Pluto | 13.2 | 2012 Mar 16 06:40:00 | 321 | B | 1 | $3.0' \times 10 \times 4.0''$ | 70 |
| 1037 | 1342241511 | Pluto | 13.2 | 2012 Mar 16 06:45:49 | 321 | G | 1 | $3.0' \times 10 \times 4.0''$ | 110 |
| 1037 | 1342241512 | Pluto | 13.2 | 2012 Mar 16 06:51:37 | 320 | G | 1 | $3.0' \times 10 \times 4.0''$ | 70 |
| 1038 | 1342241620 | Pluto | 12.5 | 2012 Mar 17 00:09:11 | 466 | B | 1 | $3.0' \times 10 \times 4.0''$ | 110 |
| 1038 | 1342241621 | Pluto | 12.5 | 2012 Mar 17 00:16:13 | 321 | B | 1 | $3.0' \times 10 \times 4.0''$ | 70 |
| 1038 | 1342241622 | Pluto | 12.5 | 2012 Mar 17 00:22:02 | 321 | G | 1 | $3.0' \times 10 \times 4.0''$ | 110 |
| 1038 | 1342241623 | Pluto | 12.5 | 2012 Mar 17 00:27:51 | 321 | G | 1 | $3.0' \times 10 \times 4.0''$ | 70 |
| 1038 | 1342241655 | Pluto | 15.9 | 2012 Mar 17 17:22:23 | 1487 | B | 1 | $3.0' \times 10 \times 4.0''$ | 110 |
| 1038 | 1342241656 | Pluto | 11.8 | 2012 Mar 17 17:37:55 | 321 | B | 1 | $3.0' \times 10 \times 4.0''$ | 70 |
| 1038 | 1342241657 | Pluto | 11.8 | 2012 Mar 17 17:43:44 | 321 | G | 1 | $3.0' \times 10 \times 4.0''$ | 110 |
| 1038 | 1342241658 | Pluto | 11.8 | 2012 Mar 17 17:49:33 | 321 | G | 1 | $3.0' \times 10 \times 4.0''$ | 70 |
| 1039 | 1342241699 | Pluto | 16.8 | 2012 Mar 18 10:52:49 | 1714 | B | 1 | $3.0' \times 10 \times 4.0''$ | 110 |
| 1039 | 1342241700 | Pluto | 11.1 | 2012 Mar 18 11:10:15 | 321 | B | 1 | $3.0' \times 10 \times 4.0''$ | 70 |
| 1039 | 1342241701 | Pluto | 11.1 | 2012 Mar 18 11:16:04 | 321 | G | 1 | $3.0' \times 10 \times 4.0''$ | 110 |
| 1039 | 1342241702 | Pluto | 11.0 | 2012 Mar 18 11:21:53 | 321 | G | 1 | $3.0' \times 10 \times 4.0''$ | 70 |

continued on next page

Table 2: *continued*

| OD | OBSID | Target | SAA | UTC Start time | Dur. | Fil. | Rep. | ScanLeg × n × cross | angle |
|------|------------|--------|------|----------------------|------|------|------|---------------------|-------|
| 1040 | 1342241865 | Pluto | 10.4 | 2012 Mar 19 04:40:59 | 559 | B | 1 | 3.0' × 10 × 4.0'' | 110 |
| 1040 | 1342241866 | Pluto | 10.3 | 2012 Mar 19 04:48:47 | 321 | B | 1 | 3.0' × 10 × 4.0'' | 70 |
| 1040 | 1342241867 | Pluto | 10.4 | 2012 Mar 19 04:54:36 | 321 | G | 1 | 3.0' × 10 × 4.0'' | 110 |
| 1040 | 1342241868 | Pluto | 10.3 | 2012 Mar 19 05:00:25 | 321 | G | 1 | 3.0' × 10 × 4.0'' | 70 |
| 1040 | 1342241928 | Pluto | 16.5 | 2012 Mar 19 20:33:06 | 1713 | B | 1 | 3.0' × 10 × 4.0'' | 110 |
| 1040 | 1342241929 | Pluto | 9.7 | 2012 Mar 19 20:50:32 | 321 | B | 1 | 3.0' × 10 × 4.0'' | 70 |
| 1040 | 1342241930 | Pluto | 9.7 | 2012 Mar 19 20:56:21 | 321 | G | 1 | 3.0' × 10 × 4.0'' | 110 |
| 1040 | 1342241931 | Pluto | 9.7 | 2012 Mar 19 21:02:10 | 321 | G | 1 | 3.0' × 10 × 4.0'' | 70 |

Acknowledgements

This work has dedicatedly been supported by European Union's Horizon 2020 Research and Innovation Programme, under Grant Agreement no 687378.

References

- Balog, Z., Müller, T.G., Nielbock, M., et al., 2014, Experimental Astronomy, 37, 129
- Kiss, Cs.; Szabó, Gy.; Horner, J., et al., 2013, A&A, 555, A3
- Kiss, C.; Müller, T. G.; Vilenius, E.; et al., 2014, Experimental Astronomy, 37, 161
- Kiss, C., Müller, T. G., Varga-Verebélyi, E., 2017, 'User Provided Data Products from the "TNOs are Cool! A Survey of the trans-Neptunian Region" Herschel Open Time Key Program', Release Note V1.0, Herschel Science Archive
- Müller, T.G., Lellouch, E., Böhnhardt, H., et al., 2009, EM&P, 105, 209
- Ott, S., 2010, "The Herschel Data Processing System — HIPE and Pipelines — Up and Running Since the Start of the Mission" in: Astronomical Data Analysis Software and Systems XIX., eds. Y. Mizumoto, K.-I. Morita, & M. Ohishi, ASP Conf. Ser., 434, 139
- Pál, A.; Kiss, Cs.; Horner, J.; et al., 2015, A&A, 583, A93
- Pilbratt, G. L., Riedinger, J. R., Passvogel, T., et al., 2010, A&A, 518, L1
- Poglitsch, A., Waelkens, C., Geis, N., et al., 2010, A&A, 518, L2
- Popesso, P.; Magnelli, B.; Buttiglione, S., et al., 2012, "The effect of the high-pass filter data reduction technique on the Herschel PACS Photometer PSF and noise", arXiv:1211.4257

Appendix

Summary of additional FITS keywords

| | |
|----------------------------------|--|
| OBS_ID | Herschel observation identifier number / single observation used for data product |
| OBSID001, OBSID002, ... OBSIDnnn | Herschel observation identifier number / multiple observations used for data product |
| PROPOSAL | Herschel proposal ID of the observations used |
| LAYER0, LAYER1 | Type of data in a specific data layer of the FITS cube ("image" or "coverage") |
| EQLEVEL | Equivalent level of SPG processing |
| TARGET | Name or designation of the target |
| INSTRUME | Main Herschel instrument |
| SUBINSTR | Subinstrument |
| FILTER | Nominal wavelength of the filter used (mircometer) |
| DATAPRID | Type of data product |
| OBSJDSTA | Start date (JD) of the first OBSID used (combined products) |
| OBSJDEND | End date (JD) of the last OBSID used (combined product) |
| JDSTART | Start (JD) of the observation block (selected repetitions) |
| JD_END | End (JD) of the observation block (selected repetitions) |
| REPETnnn | ID of the repetitions used (counting starts at 1) |
| BGIMAGE | Name of the image FITS file used for background correction |

Table 3: List of keywords added to the header of the data product FITS files. Note that not all keywords apply to a specific data product type.

List of data products provided with this release note

| target | product (FITS file) | product type | band | number of files |
|--------------|--|--------------|------|-----------------|
| 136199 Eris | map_1342224854_136199_Eris_LCDIFF_160_nm=10_sr=[001,011,...051].fits | LCDIFF | 160 | 6 |
| | map_1342224854_136199_Eris_STACKED_100_nm=23_sr=001.fits | STACKED | 100 | 1 |
| | map_1342224855_136199_Eris_LCDIFF_160_nm=10_sr=[001,011,...051].fits | LCDIFF | 160 | 6 |
| | map_1342238741_1342238742_Eris_Background_LCBG_100.fits | LCBG | 100 | 1 |
| | map_1342238741_1342238742_Eris_Background_LCBG_160.fits | LCBG | 160 | 1 |
| | map_1342238743_136199_Eris_LCALL_070_nm=15_sr=001.fits | LCALL | 070 | 1 |
| | map_1342238743_136199_Eris_LCALL_160_nm=15_sr=001.fits | LCALL | 160 | 1 |
| | map_1342238743_136199_Eris_LCDIFF_070_nm=3_sr=[001,002,...013].fits | LCDIFF | 070 | 13 |
| | map_1342238743_136199_Eris_LCDIFF_160_nm=3_sr=[001,002,...013].fits | LCDIFF | 160 | 13 |
| | map_1342238743_136199_Eris_LCDIFF_160_nm=6_sr=[001,004,...010].fits | LCDIFF | 160 | 4 |
| | map_1342238743_136199_Eris_LCMAIN_070_nm=3_sr=[001,002,...013].fits | LCMAIN | 070 | 13 |
| | map_1342238743_136199_Eris_LCMAIN_160_nm=3_sr=[001,002,...013].fits | LCMAIN | 160 | 13 |
| | map_1342238743_136199_Eris_LCMAIN_160_nm=6_sr=[001,004,...010].fits | LCMAIN | 160 | 4 |
| | map_1342238744_136199_Eris_LCALL_070_nm=15_sr=001.fits | LCALL | 070 | 1 |
| | map_1342238744_136199_Eris_LCALL_160_nm=15_sr=001.fits | LCALL | 160 | 1 |
| | map_1342238744_136199_Eris_LCDIFF_070_nm=3_sr=[001,002,...013].fits | LCDIFF | 070 | 13 |
| | map_1342238744_136199_Eris_LCDIFF_160_nm=3_sr=[001,002,...013].fits | LCDIFF | 160 | 13 |
| | map_1342238744_136199_Eris_LCDIFF_160_nm=6_sr=[001,004,...010].fits | LCDIFF | 160 | 4 |
| | map_1342238744_136199_Eris_LCMAIN_070_nm=3_sr=[001,002,...013].fits | LCMAIN | 070 | 13 |
| | map_1342238744_136199_Eris_LCMAIN_160_nm=3_sr=[001,002,...013].fits | LCMAIN | 160 | 13 |
| | map_1342238744_136199_Eris_LCMAIN_160_nm=6_sr=[001,004,...010].fits | LCMAIN | 160 | 4 |
| | map_1342238863_136199_Eris_LCALL_070_nm=15_sr=001.fits | LCALL | 070 | 1 |
| | map_1342238863_136199_Eris_LCALL_160_nm=15_sr=001.fits | LCALL | 160 | 1 |
| | map_1342238863_136199_Eris_LCDIFF_070_nm=3_sr=[001,002,...013].fits | LCDIFF | 070 | 13 |
| | map_1342238863_136199_Eris_LCDIFF_160_nm=3_sr=[001,002,...013].fits | LCDIFF | 160 | 13 |
| | map_1342238863_136199_Eris_LCDIFF_160_nm=6_sr=[001,004,...010].fits | LCDIFF | 160 | 4 |
| | map_1342238863_136199_Eris_LCMAIN_070_nm=3_sr=[001,002,...013].fits | LCMAIN | 070 | 13 |
| | map_1342238863_136199_Eris_LCMAIN_160_nm=3_sr=[001,002,...013].fits | LCMAIN | 160 | 13 |
| | map_1342238863_136199_Eris_LCMAIN_160_nm=6_sr=[001,004,...010].fits | LCMAIN | 160 | 4 |
| | map_1342238864_136199_Eris_LCALL_070_nm=15_sr=001.fits | LCALL | 070 | 1 |
| | map_1342238864_136199_Eris_LCALL_160_nm=15_sr=001.fits | LCALL | 160 | 1 |
| | map_1342238864_136199_Eris_LCDIFF_070_nm=3_sr=[001,002,...013].fits | LCDIFF | 070 | 13 |
| | map_1342238864_136199_Eris_LCDIFF_160_nm=3_sr=[001,002,...013].fits | LCDIFF | 160 | 13 |
| | map_1342238864_136199_Eris_LCDIFF_160_nm=6_sr=[001,004,...010].fits | LCDIFF | 160 | 4 |
| | map_1342238864_136199_Eris_LCMAIN_070_nm=3_sr=[001,002,...013].fits | LCMAIN | 070 | 13 |
| | map_1342238864_136199_Eris_LCMAIN_160_nm=3_sr=[001,002,...013].fits | LCMAIN | 160 | 13 |
| | map_1342238864_136199_Eris_LCMAIN_160_nm=6_sr=[001,004,...010].fits | LCMAIN | 160 | 4 |
| 50000 Quaoar | map_1342229967_50000_Quaoar_LCALL_100_nm=82_sr=001.fits | LCALL | 100 | 1 |
| | map_1342229967_50000_Quaoar_LCALL_160_nm=82_sr=001.fits | LCALL | 160 | 1 |
| | map_1342229967_50000_Quaoar_LCDIFF_100_nm=3_sr=[001,002,...080].fits | LCDIFF | 100 | 80 |
| | map_1342229967_50000_Quaoar_LCDIFF_160_nm=3_sr=[001,002,...080].fits | LCDIFF | 160 | 80 |
| | map_1342229967_50000_Quaoar_LCDIFF_160_nm=6_sr=[001,004,...076].fits | LCDIFF | 160 | 26 |
| | map_1342229967_50000_Quaoar_LCMAIN_100_nm=3_sr=[001,002,...080].fits | LCMAIN | 100 | 80 |
| | map_1342229967_50000_Quaoar_LCMAIN_160_nm=3_sr=[001,002,...080].fits | LCMAIN | 160 | 80 |
| | map_1342229967_50000_Quaoar_LCMAIN_160_nm=6_sr=[001,004,...076].fits | LCMAIN | 160 | 26 |
| | map_1342230064_50000_Quaoar_LCALL_100_nm=82_sr=001.fits | LCALL | 100 | 1 |
| | map_1342230064_50000_Quaoar_LCALL_160_nm=82_sr=001.fits | LCALL | 160 | 1 |
| | map_1342230064_50000_Quaoar_LCDIFF_100_nm=3_sr=[001,002,...080].fits | LCDIFF | 100 | 80 |
| | map_1342230064_50000_Quaoar_LCDIFF_160_nm=3_sr=[001,002,...080].fits | LCDIFF | 160 | 80 |
| | map_1342230064_50000_Quaoar_LCDIFF_160_nm=6_sr=[001,004,...076].fits | LCDIFF | 160 | 26 |
| | map_1342230064_50000_Quaoar_LCMAIN_100_nm=3_sr=[001,002,...080].fits | LCMAIN | 100 | 80 |
| | map_1342230064_50000_Quaoar_LCMAIN_160_nm=3_sr=[001,002,...080].fits | LCMAIN | 160 | 80 |
| | map_1342230064_50000_Quaoar_LCMAIN_160_nm=6_sr=[001,004,...076].fits | LCMAIN | 160 | 26 |
| | map_1342230111_50000_Quaoar_LCALL_100_nm=82_sr=001.fits | LCALL | 100 | 1 |
| | map_1342230111_50000_Quaoar_LCALL_160_nm=82_sr=001.fits | LCALL | 160 | 1 |
| | map_1342230111_50000_Quaoar_LCDIFF_100_nm=3_sr=[001,002,...080].fits | LCDIFF | 100 | 80 |
| | map_1342230111_50000_Quaoar_LCDIFF_160_nm=3_sr=[001,002,...080].fits | LCDIFF | 160 | 80 |
| | map_1342230111_50000_Quaoar_LCDIFF_160_nm=6_sr=[001,004,...076].fits | LCDIFF | 160 | 26 |
| | map_1342230111_50000_Quaoar_LCMAIN_100_nm=3_sr=[001,002,...080].fits | LCMAIN | 100 | 80 |
| | map_1342230111_50000_Quaoar_LCMAIN_160_nm=3_sr=[001,002,...080].fits | LCMAIN | 160 | 80 |
| | map_1342230111_50000_Quaoar_LCMAIN_160_nm=6_sr=[001,004,...076].fits | LCMAIN | 160 | 26 |

